

On Higher-Order Representations of Polyphase-Coded FM Radar Waveforms

Peng Seng Tan, John Jakobosky, James M. Stiles and Shannon D. Blunt
Radar Systems Lab, University of Kansas, Lawrence, KS

Abstract—It has recently been shown that arbitrary polyphase codes can be implemented as FM waveforms through a radar-specific version of the Continuous Phase Modulation (CPM) framework. These waveforms, denoted as Polyphase-Coded FM (PCFM) can be viewed as a first-order hold representation of the phase function (where traditional codes represent a zero-order hold). Here we examine higher-order representations as a means to achieve further variety over the space of possible waveform functions one may optimize. Specifically, the relationships between the first, second, and third-order representations are considered, along with the optimization of the coding for each.

I. INTRODUCTION

The combination of increasing demand for radio frequency (RF) spectrum [1,2] and the push for greater design freedom, enhanced sensitivity, and new sensing modalities has yielded myriad contributions to the burgeoning field of waveform diversity [3,4,5]. While there has been considerable work on the design of radar codes (e.g. [6] and references therein) it is only recently that the implementation of arbitrary codes has been realized in a power and spectrally efficient manner via a radar-specific form of Continuous Phase Modulation (CPM) [7]. This scheme, denoted as polyphase-code FM (PCFM), converts codes into FM waveforms in a manner akin to first-order hold in the phase domain. Here this implementation is generalized to higher-order representations to further expand the possible design space for optimization.

In essence, this generalization enables new ways in which to represent nonlinear FM (NLFM) waveforms where, in theory, there are infinite possible continuous phase functions that may exist, even for a finite pulse width and bandwidth. Because they can provide low range sidelobes without the need for amplitude tapering and are naturally well-suited to high-power transmitters, many different approaches have emerged for the design of NLFM waveforms [8-13]. However, given the growing ubiquity of high performance computing and parallel processing it stands to reason that NLFM waveforms based upon some underlying coding representation may provide the means with which to achieve unprecedented performance by searching the high dimensional parameter space [14, 15]. As such, of particular interest is the determination of new and useful mappings from a discrete code into a continuous FM waveform. Recent contributions include [16] based on a constellation-constrained version of CPM that leverages the Laurent decomposition and [17] that demonstrates the use of parameterized Bezier curves for FM waveform design.

The higher-order PCFM representation described here was inspired by the polynomial phase functions proposed by Doerry [13]. Table I provides a general comparison between the different orders (1st and higher) and also includes polyphase codes themselves as a notional zero-order representation.

TABLE I. WAVEFORM REPRESENTATIONS

Waveform representation	Equivalent approaches in radar waveform generation
0th order	Discrete codes (e.g. P3); abrupt phase transitions
1st order	PCFM via [7]; linear phase trajectories
2nd order	LFM and NLFM; quadratic phase trajectories
3 rd order & Higher	Higher orders of NLFM

II. HIGHER-ORDER PCFM IMPLEMENTATIONS

In [7] the CPM implementation used for power and spectrally efficient communications was modified to enable the implementation of arbitrary polyphase codes as FM radar waveforms. The resulting polyphase-coded FM (PCFM) scheme is inherently a first-order representation that can be expressed as

$$\phi_1(t) = \int_0^t \left[\sum_{n=1}^N \alpha_n g_1(\tau - (n-1)T_p) \right] d\tau + \phi_{1,0} \quad (1)$$

where α_n for $n=1, 2, \dots, N$ are a first-order code that may or may not be derived from a zero-order polyphase code of length $N+1$, $g_1(\tau)$ is a shaping filter as defined in [7] to have time support on $[0, T_p]$ for pulse width $T = NT_p$, and $\phi_{1,0}$ is the initial phase for this first-order representation.

If we now define the first-order coded function $a(\tau)$ as

$$a(\tau) = \sum_{n=1}^N \alpha_n g_1(\tau - (n-1)T_p), \quad (2)$$

which represents the time-varying frequency of the waveform, then (1) becomes

$$\phi_1(t) = \int_0^t a(\tau) d\tau + \phi_{1,0}. \quad (3)$$

Using this format, general expressions for second-order and third-order representations can readily be defined as

$$\phi_2(t) = \int_0^t \int_0^{\tau} b(\tau') d\tau' d\tau + \int_0^t \omega_{2,0} d\tau + \phi_{2,0} \quad (4)$$

and

$$\phi_3(t) = \int_0^t \int_0^{\tau} \int_0^{\tau'} c(\tau'') d\tau'' d\tau' d\tau + \int_0^t \int_0^{\tau} \beta_{3,0} d\tau' d\tau + \int_0^t \omega_{3,0} d\tau + \phi_{3,0} \quad (5)$$

respectively, where $\phi_{2,0}$ and $\omega_{2,0}$ are the initial phase and frequency for the second-order implementation and $\phi_{3,0}$, $\omega_{3,0}$, and $\beta_{3,0}$ are the initial phase, frequency, and chirp-rate for the third-order implementation. The term $b(\tau')$ in (4) is the second-order coded function defined as

$$b(\tau') = \sum_{n=1}^N b_n g_2(\tau' - (n-1)T_p) \quad (6)$$

representing the time-varying chirp-rate where b_n for $n=1, 2, \dots, N$ is the second-order code and $g_2(\tau')$ the associated second-order shaping filter. Likewise,

$$c(\tau'') = \sum_{n=1}^N c_n g_3(\tau'' - (n-1)T_p) \quad (7)$$

is the third-order coded function representing time-varying *chirp-acceleration* according to c_n for $n=1, 2, \dots, N$ and $g_3(\tau'')$ the third-order shaping filter.

Further, it is possible for these implementations to be combined. For example, the first-order coding may be incorporated into the second-order implementation as

$$\phi_2(t) = \int_0^t \int_0^{\tau} b(\tau') d\tau' d\tau + \int_0^t a(\tau) d\tau + \phi_{2,0}. \quad (8)$$

Likewise, both first and second-order coding can be incorporated as

$$\phi_3(t) = \int_0^t \int_0^{\tau} \int_0^{\tau'} c(\tau'') d\tau'' d\tau' d\tau + \int_0^t \int_0^{\tau} b(\tau') d\tau' d\tau + \int_0^t a(\tau) d\tau + \phi_{3,0} \quad (9)$$

into the third-order implementation. In the same spirit as the ‘‘over-coding’’ scheme introduced in [15], there is a richness to this higher-order framework that provides the possibility for different phase functions to be realized, thus enabling greater design freedom.

It is important to note that additional care must be taken when using higher-order coding. For example, in [7] it was stated that the shaping filter $g_1(\tau)$ should integrate to unity at the end of its time support on $[0, T_p]$ and that the permissible values of α_n exist on $[-\pi, \pi]$ (though the latter was relaxed somewhat in [15]). The combination of these factors limit the degree of phase change (to $|\pi|$) over the time interval T_p , which subsequently serves to constrain the (angular) bandwidth to

$$\pm \frac{\pi}{T_p} = \pm \frac{\pi N}{T} \cong \pm \frac{\pi BT}{T} = \pm \pi B \text{ rad/s}, \quad (10)$$

or simply $\pm B/2$ Hz, where we have used the relationship $T = NT_p$ and the fact that the time-bandwidth product BT is well approximated by N . Note that (10) is a baseband expression. Imposing this same constraint using the second and third-order representations requires that the compounding effect of the additional integration stages be taken into account, which impacts the selection of the coding values for b_n and c_n as well as the associated shaping filters $g_2(\tau)$ and $g_3(\tau)$.

To understand the relationship between the first, second, and third-order representations consider how each could be used to implement a standard LFM waveform that is known to possess a constant chirp-rate. For 3-dB bandwidth B and pulse width T , the LFM chirp-rate is simply

$$\beta_{\text{LFM}} = \frac{B}{T} \quad (11)$$

and the time-bandwidth product is $BT = \beta_{\text{LFM}} T^2$. Likewise, since the LFM phase is known to be quadratic in time this waveform clearly requires a second-order component to be perfectly represent (a first-order LFM approximation was presented in [7]). Assuming an up-chirp at baseband, the initial frequency is $\omega_{2,0} = -\pi/T_p$ and the final frequency at the end of the pulse is $+\pi/T_p$, with the initial phase $\phi_{2,0}$ being arbitrary. Thus the LFM waveform traverses $2\pi/T_p$ of angular bandwidth, or $B = 1/T_p \cong N/T$, and so from (11) we obtain $\beta_{\text{LFM}} = N/T^2 = b_n$ for use with the shaping filter $g_2(\tau) = \text{rect}[0, T_p]$ in (6). Note that, as one would expect, b_n is a constant to realize a LFM waveform.

Now consider the LFM implementation using the third-order representation of (5) and (7). The most straightforward way would be to set the chirp-rate as $\beta_{3,0} = \beta_{\text{LFM}} = N/T^2$ and the initial frequency as $\omega_{3,0} = \omega_{2,0} = -\pi/T_p$ with initial phase $\phi_{3,0}$ again arbitrary, which is simply the second-order representation above. Alternatively, note that the derivative of the rectangular shaping filter with time support on $[0, T_p]$ results in a positive unit impulse function $\delta(\tau'')$ at $\tau''=0$ and a negative unit impulse function $-\delta(\tau''-T_p)$ at $\tau''=T_p$. Therefore, based on the construction in (7) it is observed that all the impulses will cancel except for the first positive impulse at the beginning of the pulse and last negative impulse at the end of the pulse. As a result, (7) for the LFM waveform can be simplified to

$$c(\tau'') = \frac{N}{T^2} [\delta(\tau'') - \delta(\tau'' - T)] \quad (12)$$

with $\beta_{3,0} = 0$ and the other parameters unchanged. As shown in Fig. 1, this third-order implementation has an identical spectral content to that of the second-order implementation above, as expected.

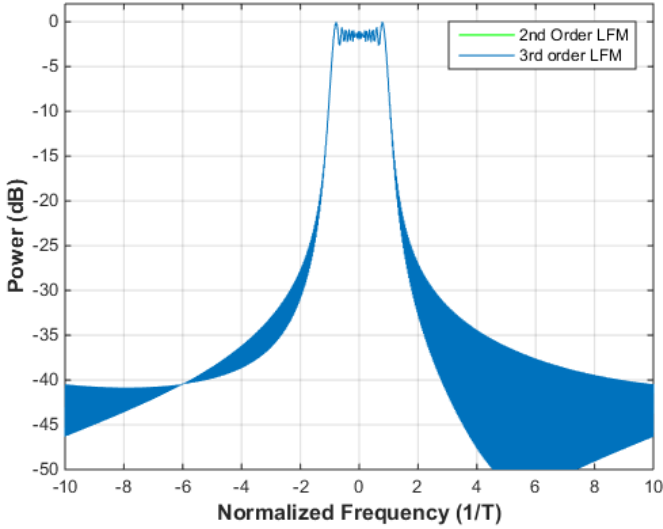


Figure 1. Spectral content of 2nd order and 3rd order implementations of LFM with $BT = 64$

A nearly identical relationship exists between the first-order and second-order representations to implement a piece-wise approximation to LFM. The point of this overly elaborate means of implementing a common waveform is that different order representations can map into the same waveform, albeit through different constructions. Conversely, and more importantly, these higher-order components provide new phase trajectories which can be exploited as additional degrees-of-freedom in waveform design without necessarily increasing the time-bandwidth product (again, in the same spirit as [15]).

III. HIGHER-ORDER PCFM OPTIMIZATION

There are many ways in which to search the high-dimensional space parameterized by the PCFM codes α_n , b_n , and c_n . In [14] the *performance diversity* paradigm was introduced for the first-order representation in which the complementary nature of the cost functions for peak sidelobe level (PSL), integrated sidelobe level (ISL), and the shape of the power spectral density (because it is the Fourier transform of the autocorrelation) were used to avoid local minima in a greedy search approach to thereby discern waveforms with quite low sidelobes. The spectrum cost function takes the form of a frequency template error (FTE) relative to a Gaussian power spectral density [14]. This same performance diversity approach is also adopted here to optimize the second and third-order representations, though these also require the initial frequency and chirp-rate to be established since, unlike the arbitrary initial phase, these factors do have an impact upon waveform performance.

Figures 2-4 compare the autocorrelations, spectral content, and instantaneous frequency for 1st and 2nd order optimized waveforms of $BT = 64$. The 2nd order waveform is observed to achieve slightly more than 2 dB lower PSL than the 1st order (Fig. 2), though the 2nd order also realizes a slightly slower spectral roll-off (Fig. 3) as a result of the increased spectral excursion at the ends of the pulse (Fig. 4).

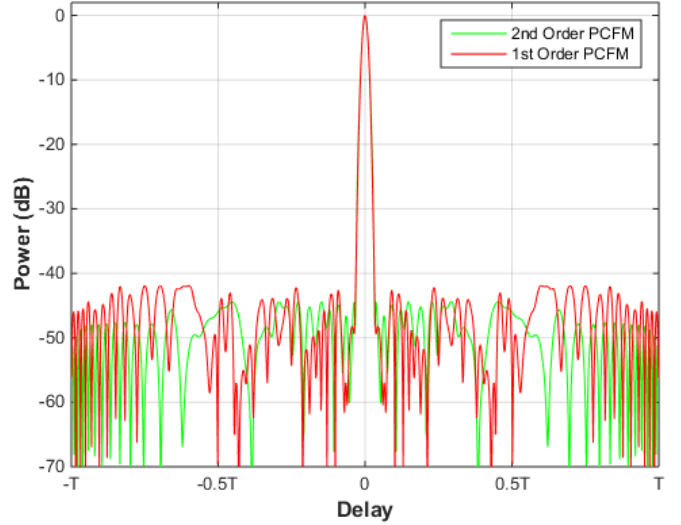


Figure 2. Autocorrelations of 1st and 2nd order optimized waveforms

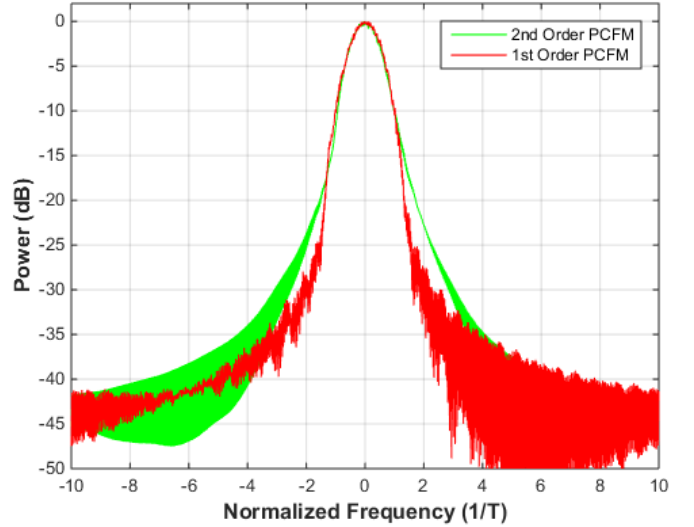


Figure 3. Spectral content of 1st and 2nd order optimized waveforms

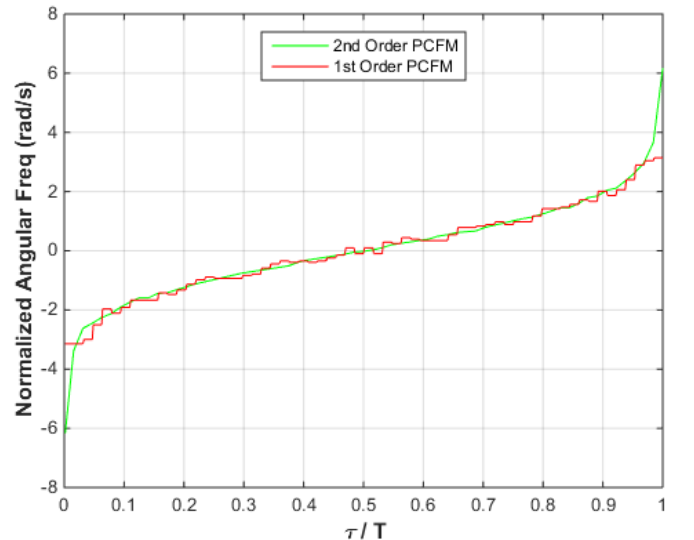


Figure 4. Instantaneous frequency of 1st and 2nd order optimized waveforms

Figures 5-7 depicts the comparison between 1st and 3rd order optimized waveforms. Here it is observed that the 1st order waveform is superior to this particular 3rd order waveform in terms of PSL by more than 5 dB (Fig. 5) with roughly the same spectral content (Fig. 6) as expected by the mostly similar frequency excursion (Fig. 7).

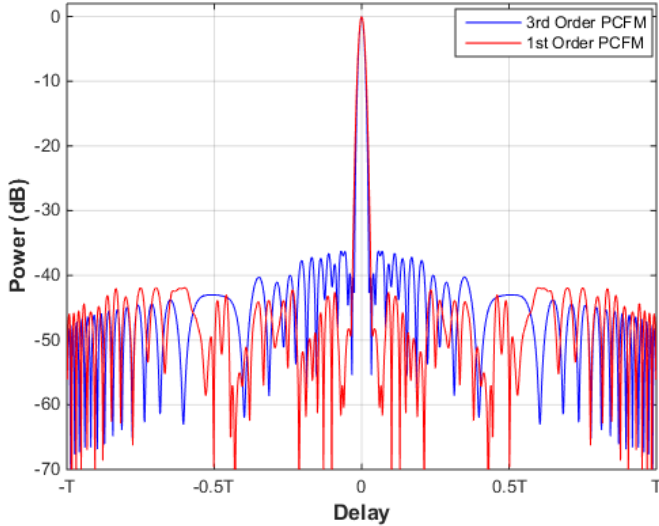


Figure 5. Autocorrelations of 1st and 3rd order optimized waveforms

Table II provides the PSL and ISL values obtained by optimizing $BT = 64$ waveforms for first, second, and third-order representations of (1), (4), and (5). It is also instructive to compare these results with the hyperbolic FM (HFM) waveform for which a PSL bound (specific to HFM) can be computed to be -39.1 dB as a function of $BT = 64$ [10,14]. From the table, 2nd order provides the lowest PSL and ISL, followed by 1st order, with both surpassing the benchmark of the HFM bound on PSL. In contrast, 3rd order does not surpass the bound and likewise for 4th order (not shown). It can thus be inferred that optimization of the time-varying chirp rate (2nd order) is preferable from a general performance standpoint.

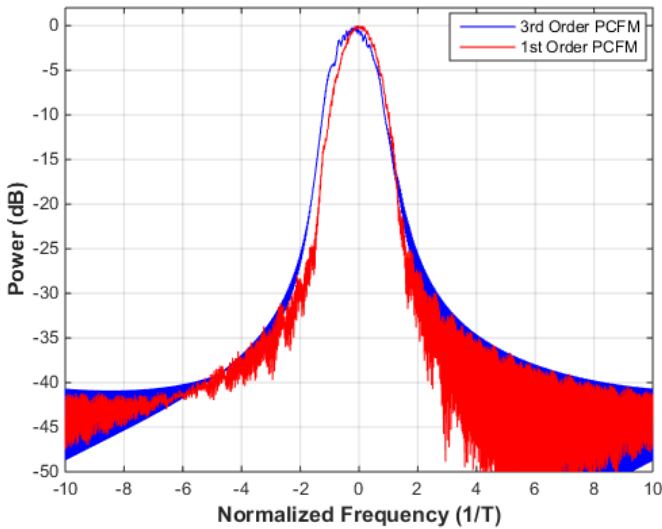


Figure 6. Spectral content of 1st and 3rd order optimized waveforms

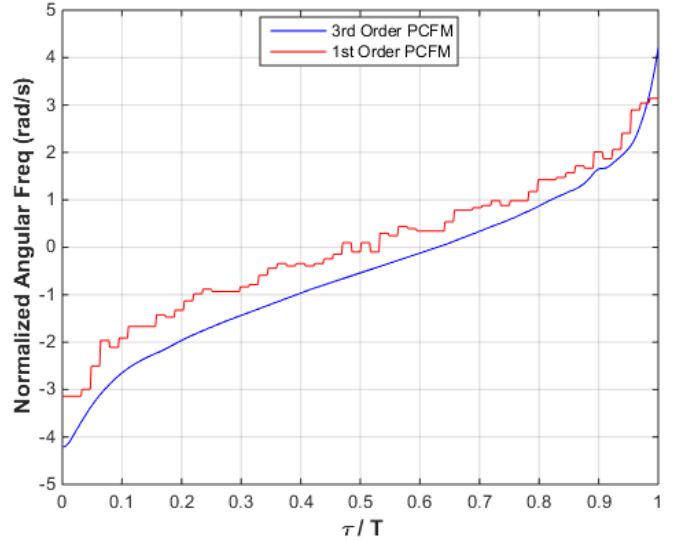


Figure 7. Instantaneous frequency of 1st and 3rd order optimized waveforms

TABLE II. PSL AND ISL FOR 1ST, 2ND AND 3RD ORDER OPTIMIZED WAVEFORMS FOR $BT = 64$

	1 st order	2 nd order	3 rd order	HFM bound
PSL (dB)	-41.91	-44.39	-36.25	-39.1
ISL (dB)	-57.38	-59.34	-53.86	N/A

For the optimization results shown above, the 1st order representation was initialized so the α_n values approximate an LFM, which has been found to yield good final results due to consolidation of waveform ambiguity in the range-Doppler ridge. The 2nd order optimization permitted initialization with the scaled inverse of Taylor window coefficients (Fig. 8) corresponding to -40 dB range sidelobes. The piece-wise difference of these coefficients (approximating the derivative) was used for 3rd order initialization.

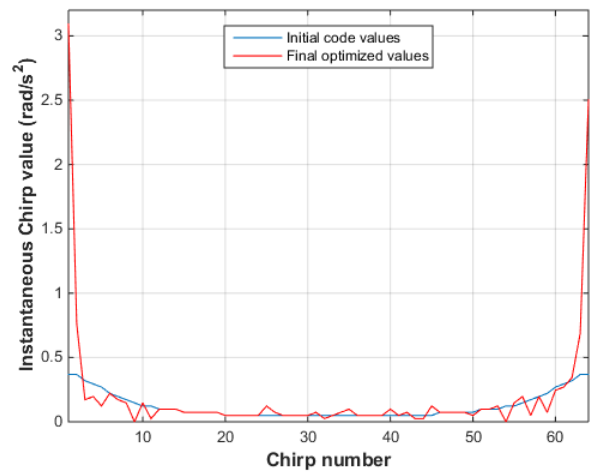


Figure 8. Initial code versus optimized values for the 2nd order PCFM waveform

IV. MIXED-ORDER PCFM OPTIMIZATION

Using (8) and (9) the different implementation orders can be combined for optimization, with the resulting increase in available degrees-of-freedom expected to further improve performance. We consider both sequential and joint optimization of the 1st, 2nd, and 3rd orders with BT kept fixed at 64 for the sake of comparison. Sequential optimization is accomplished by selecting a particular order (say the 2nd) and performing optimization until no further improvement is possible, freezing the associated coding values (here b_n for $n=1, 2, \dots, N$) and then optimizing the waveform with the inclusion of another order (1st or 3rd). At the first stage the code values for the latter order(s) to be optimized are set to 0. Sequential optimization is clearly more computationally efficient than joint optimization, though the latter can generally be expected to yield waveforms with lower sidelobes.

Figures 9-11 depicts the autocorrelations, spectral content, and instantaneous frequency of the jointly optimized waveforms. Compared the best previous case (2nd order) in Fig. 2, the use of multiple orders certainly provides enhanced sensitivity. Also, while the instantaneous frequency in Fig. 11 still possesses the general shape one expects from a good NLFM waveform, it is important to note the small perturbations that result from optimization and that provide some of the performance enhancement.

Table III provides the PSL and ISL values obtained when performing sequential and joint optimization on the mixed-order implementations in (8) and (9). It is observed that joint optimization is nominally better than sequential optimization, though perhaps not enough so to justify the increased computation requirement. Based on different combinations it was also observed that the preferred ordering for sequential optimization is to begin with 2nd order, with little difference regarding whether 1st or 3rd order occurs next. Comparing to the best results in Table II (2nd order), it is also noted that the mixed-order representations yield improvement of roughly 4 dB in PSL and 6 dB in ISL. Thus there is clearly a benefit to combining the orders. Further, there is observed to be a benefit, albeit small, to using the 3rd order as it provides a PSL improvement of 0.20 dB and 0.22 dB for the sequential and joint optimization results, respectively.

TABLE III. PSL AND ISL FOR SEQUENTIAL AND JOINT OPTIMIZATION OF MULTIPLE ORDERS FOR $BT = 64$

	Seq. 2nd & 1st orders	Joint 2nd & 1st orders	Seq. 2 nd , 1 st , & 3 rd orders	Joint 2 nd , 1 st , & 3 rd orders
PSL (dB)	-48.25	-48.43	-48.45	-48.65
ISL (dB)	-64.25	-64.83	-64.60	-65.47

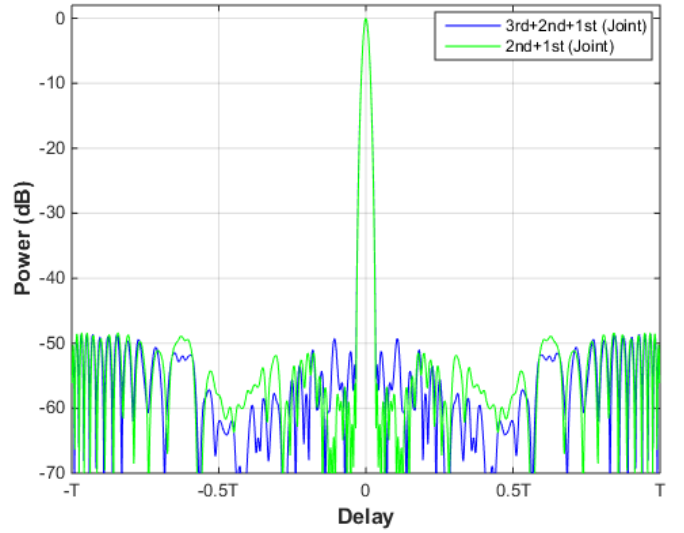


Figure 9. Autocorrelations of jointly optimized waveforms via (8) and (9)

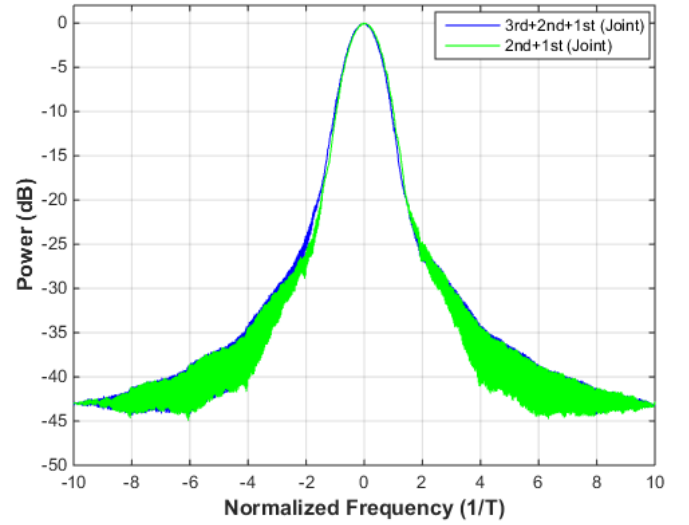


Figure 10. Spectral content of jointly optimized waveforms via (8) and (9)

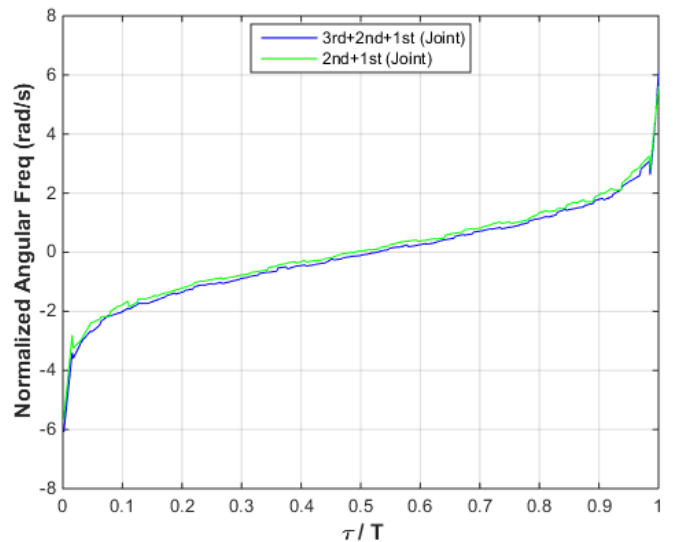


Figure 11. Instantaneous freq. of jointly optimized waveforms via (8) and (9)

V. CONCLUSIONS

In this paper, we have extended the 1st order representation of polyphase-coded FM (PCFM) to higher orders so as to exploit the additional degrees-of-freedom these higher orders provide without any increase in time-bandwidth product. Simulation results have shown that optimization of the 2nd order representation yields about 2.5 dB lower PSL compared to the previous 1st order optimization. Further, an additional 4 dB PSL improvement is observed when 1st and 2nd orders are optimized jointly, with 3rd order providing a small additional enhancement. While joint optimization of multiple orders does, as expected, result in better performance than sequential optimization of the different orders, the difference is nominal thus implying that the lower computational requirement for sequential optimization may be preferable when the goal is to design high time-bandwidth product waveforms.

REFERENCES

- [1] H. Griffiths, L. Cohen, S. Watts, E. Mokole, C. Baker, M. Wicks, and S. Blunt, "Radar spectrum engineering and management: technical and regulatory issues," *Proc. IEEE*, vol. 103, no. 1, pp. 85-102, Jan. 2015.
- [2] H. Griffiths, S. Blunt, L. Cohen, and L. Savy, "Challenge problems in spectrum engineering and waveform diversity," *IEEE Radar Conf.*, Ottawa, Canada, 29 Apr. – 3 May 2013.
- [3] M. Wicks, E. Mokole, S.D. Blunt, V. Amuso, and R. Schneible, eds., *Principles of Waveform Diversity & Design*, SciTech Publishing, 2010.
- [4] S. Pillai, K.Y. Li, I. Selesnick, and B. Himed, *Waveform Diversity: Theory & Applications*, McGraw-Hill, 2011.
- [5] F. Gini, A. De Maio, and L.K. Patton, *Waveform Design and Diversity for Advanced Radar Systems*, IET, 2012.
- [6] N. Levanon and E. Mozeson, *Radar Signals*, Wiley-IEEE Press, 2004.
- [7] S.D. Blunt, M. Cook, J. Jakobosky, J. de Graaf, and E. Perrins, "Polyphase-coded FM (PCFM) radar waveforms, part I: implementation," *IEEE Trans. Aerospace & Electronic Systems*, vol. 50, no. 3, pp. 2218-2229, July 2014.
- [8] C.E. Cook, "A class of nonlinear FM pulse compression signals," *Proc. IEEE*, vol. 52, no. 11, pp. 1369-1371, Nov. 1964.
- [9] J.A. Johnston and A.C. Fairhead, "Waveform design and Doppler sensitivity analysis for nonlinear FM chirp pulses," *IEE Proc. F – Communications, Radar & Signal Processing*, vol. 133, no. 2, pp. 163-175, Apr. 1986.
- [10] T. Collins and P. Atkins, "Nonlinear frequency modulation chirps for active sonar," *IEE Proc. Radar, Sonar & Navigation*, vol. 146, no. 6, pp. 312-316, Dec. 1999.
- [11] I. Gladkova, "Design of frequency modulated waveforms via the Zak transform," *IEEE Trans. Aerospace & Electronic Systems*, vol. 40, no. 1, pp. 355-359, Jan. 2004.
- [12] E. De Witte and H.D. Griffiths, "Improved ultra-low range sidelobe pulse compression waveform design," *Electronics Letters*, vol. 40, no. 22, pp. 1448-1450, Oct. 2004.
- [13] A.W. Doerry, "Generating nonlinear FM chirp waveforms for radar," *Sandia Report*, SAND2006-5856, Sept. 2006.
- [14] S.D. Blunt, J. Jakobosky, M. Cook, J. Stiles, S. Seguin, and E.L. Mokole, "Polyphase-coded FM (PCFM) radar waveforms, part II: optimization," *IEEE Trans. Aerospace & Electronic Systems*, vol. 50, no. 3, pp. 2230-2241, July 2014.
- [15] J. Jakobosky, S.D. Blunt, and Braham Himed, "Optimization of 'over-coded' radar waveforms," *IEEE Radar Conf.*, Cincinnati, OH, 19-23 May 2014.
- [16] R.F. Tigrek and U.C. Doyuran, "Utilization of Laurent decomposition for CPM radar waveform design," *IEEE Radar Conf.*, Ottawa, Canada, 29 Apr. – 3 May 2013.
- [17] J. Kurdzo, B.L. Cheong, R. Palmer, and G. Zhang, "Optimized NLFM pulse compression waveforms for high-sensitivity radar observations," *Intl. Radar Conf.*, Lille, France, 13-17 Oct. 2014.